



Hydrophobic membranes for salts recovery from desalination plants

Francesca Macedonio^{a,b*}, Enrico Drioli^{a,b}

^aDepartment of Chemical Engineering and Materials, University of Calabria, Via P. Bucci Cubo 44/A, 87036 Arcavacata di Rende (CS), Italy

^bInstitute on Membrane Technology, ITM-CNR, c/o University of Calabria, Via P. Bucci Cubo 17/C, 87036 Arcavacata di Rende (CS), Italy

Tel.: +39 0984 492014; Fax: +39 0984 402103; e-mail: macedonio@unical.it

Received 3 June 2009; Accepted 18 December 2009

ABSTRACT

Membrane crystallization (MCr) can be used to process highly concentrated aqueous solutions. In MCr, membrane distillation is used to recover water and to generate the desired supersaturation in a crystallizer tank where crystals can be precipitated. In this paper the stability and control of MCr process has been investigated. The experimental tests have been carried out on streams representing nanofiltration and reverse osmosis retentate streams of the desalination plants. The deposition and accumulation of crystals on membrane surface and inside the membrane module has been prevented by recovering the produced crystals and by controlling the temperature of the solution flowing along the membrane module. The obtained almost constant trend of the trans-membrane flux has been the demonstration of the good carried out operations. The produced particles have been characterized in terms of shape, dimension, crystal size distribution (CSD), coefficient of variation (CV) and growth rate. The obtained CVs are lower than those from conventional equipments. Therefore, they are characteristic of narrow CSD and of qualitatively better products. Moreover, the experimentally determined crystals growth rate has allowed (i) to study the fluid-dynamic effect on MCr operation, (ii) to determine the crystals growth control based mechanism and (iii) to show that the presence of ions accelerates kinetic rate of NaCl crystallization while the presence of humic acid (the main component of the natural organic matter contained in waters) inhibits crystals growth rate.

Keywords: Crystals characterization; Crystals recovery; Membrane crystallizer

1. Introduction

Waters of the Ocean contain so many organic and inorganic elements that they are figuratively called 'liquid polymetallic ore.' There are more than 70 dissolved elements in marine waters and chlorine, sodium, magnesium, sulphate, calcium, potassium and bicarbonate are the main components representing more than 99% of all the dissolved salts. These waters are a reserve

of raw material for the production of fertilisers, salts, acids, alkalis, various metals and a number of chemical products; sodium chloride is the most important mineral obtained directly from seawater and Mexico leads the Pacific nations in salt extraction from the sea; Japan and California are the main sites for the extraction of magnesium, particularly used in industrial metal alloys; bromine extracted from seawater is used in the food, dye, pharmaceutical and photo industries. Reserves of chemical resources in the Ocean are practically unlimited, since the constant chemical composition of sea

*Corresponding author.

water is based upon continual deposition/solubilization from the environment. Valuable compounds can be also extracted from the highly concentrated nanofiltration (NF)/reverse osmosis (RO) retentate streams of the desalination plants due to their high concentration in chemical components. In literature, various studies can be found for the recovery of the compounds present in NF and RO retentate:

- the Murray–Darling Basin Commission, in order to reduce the environmental problem of the salinity in the Murray Basin, converts the salts present in the water in commercial products addressed to the market: first the retentate is evaporated and then it is sent to a conventional crystallizer for the extraction of NaCl and epsomite ($\text{MgSO}_4 \cdot 7\text{H}_2\text{O}$). The fine quality salts are produced at a cost of 18.49 and of 329 \$/t, respectively [1].
- Another example can be found in [2]. He suggested dual-purpose desalination-salt production systems, namely: UF-NF-MSF-crystallisation and UF-NF-RO-MSF-crystallisation. In these systems, the high rate of water recovery is accompanied by salt obtainment. Moreover, he calculated a water cost equal to \$0.71 /m³ in UF-NF-MSF-crystallisation system and \$0.43 /m³ in UF-NF-RO-MSF-crystallisation system respectively, competitive compared to those of potable water produced in thermal or RO seawater plants.

In various previous works Drioli and co-workers [3–6] proposed the recourse to membrane distillation (MD) and membrane crystallization (MCr) techniques for the exploitation of the components contained in the NF and/or RO retentate streams of the desalination plants. Membrane distillation/membrane crystallization, thanks to their intrinsic characteristic of temperature driven membrane processes, allow to produce fresh water also from highly concentrated feeds (such as the brine streams) with which NF and RO cannot operate due to the osmotic phenomena. Therefore, the introduction of a MD/MCr unit downstream RO and/or NF retentate allows to increase the overall recovery factor, thus reducing the volume of concentrated streams usually discharged by the desalination plants and, in the case of MCr, recovering the dissolved salts in the form of high-quality crystals.

In this work, the stability of the MCr operation in the treatment of NF/RO retentate streams has been studied and optimized. The produced particles have been characterized in terms of shape, dimension, crystal size distribution (CSD), coefficient of variation (CV) and growth rate. Moreover, the influence of ions and organics on the kinetic rate of the achieved particles has been analysed.

2. Control of the membrane crystallization process and description of the plant

In order to guarantee MCr proper functioning and stability, the crucial requirement is to avoid crystals formation and deposition on the membrane surface and in the membrane module.

The salts precipitation occurs when the solution is supersaturated. Unless a solution is supersaturated, crystals can neither form nor grow. Supersaturation refers to the quantity of solute present in solution compared with the quantity which would be present if the solution were kept for a very long period of time with solid phase in contact with the solution. The latter value is the equilibrium solubility at the temperature and pressure under consideration. As a consequence, the potential salts precipitation can be predicted by the comparison between the *solubility product* (K_{sp}) and the *ionic product* (IP):

- if $K_{sp} > \text{IP}$ the solution is not saturated and the precipitation doesn't occur;
- if $K_{sp} = \text{IP}$ the solution is saturated;
- if $K_{sp} < \text{IP}$ solid will precipitate until the saturation concentration is reached.

Moreover, for aiming to the production of valuable salts (such as sodium chloride and magnesium sulphate the salts naturally present in the highly NF/RO concentrated streams of the desalination plants), the exact composition of the stream fed to the MCr unit has to be known.

Because the considered NF and RO retentate streams are characterized by the composition reported in Table 1, calcium sulphate, magnesium sulphate and sodium chloride are the salts that can precipitate. All the details regarding the used membrane-based desalination plant which gave rise to the composition reported in Table 1 can be found in [6].

Table 1
NF and RO retentate composition.

Stream	RO retentate	NF retentate
Ion	Composition [g/L]	
Cl ⁻	44.89	34.47
Na ⁺	24.81	19.05
SO ₄ ²⁻	0.5831	10.38
Mg ²⁺	0.5352	4.959
Ca ²⁺	0.2488	1.384
HCO ₃ ⁻	0.1680	0.4160
K ⁺	0.8978	0.6893
CO ₃ ²⁻	0.0041	0.0103
Br ⁻	0.1886	0.0848
Total	72.32	71.44

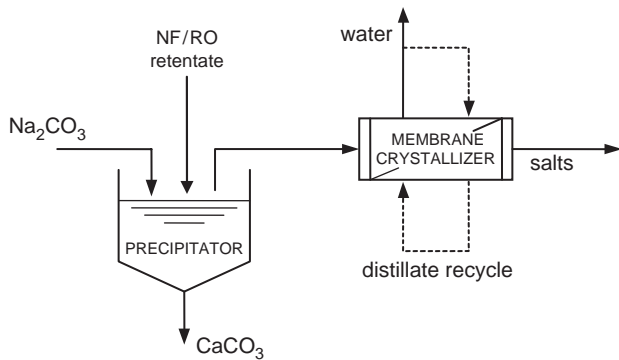


Fig. 1. Schematic flow sheet of part of the lab plant: precipitator (for the removal of Ca^{2+} ions from NF/RO retentate) and MCr (for the recovery of fresh water and salts) [6].

For what concerns *calcium sulphate*, its solubility product (K_{sp}) at 25°C is very low and equal to $7.1 \cdot 10^{-5}$ [7]. Because NF and RO retentate streams of the analysed desalination system were characterized by high calcium concentration, in order to avoid CaSO_4 precipitation during the concentration of the NF/RO brine (which can cause scaling and limits the recovery of magnesium sulphate), Ca^{2+} ions have been precipitated as CaCO_3 through reactive precipitation with anhydrous sodium carbonate. In particular, around 98% of Ca^{2+} ions have been precipitated when Na_2CO_3 was added in 1:1.05 molar ratio of $\text{Ca}^{2+}/\text{CO}_3^{2-}$. After the precipitation step, the so-treated retentate streams have been sent to a MCr in order to recover sodium chloride and magnesium sulphate (see Fig. 1).

For what concerns *magnesium sulphate*, its solubility increases with temperature ($\Delta H_{\text{sol}} = 3.18 \text{ kcal/mol}$)

and at 25°C (temperature of the crystallization tank) it precipitates as $\text{MgSO}_4 \times 7\text{H}_2\text{O}$ (epsomite) if its concentration is higher than 710 g/L . *Sodium chloride* solubility does not change much with temperature. In the range $0\text{--}100^\circ\text{C}$ it increases from 35.7 to $39.8 \text{ g NaCl/100 g H}_2\text{O}$ [8], typical behaviour of a salt with small ΔH_{sol} ($\Delta H_{\text{sol}} = 0.93 \text{ kcal/mol}$). Therefore in the crystallization tank NaCl precipitates when its concentration is higher than $36.15 \text{ g NaCl/100 g H}_2\text{O}$.

Because the solubility of solids in solution is sensitive to changes in temperature (whose effect on salt solubility depends on its *enthalpy change of solution*, ΔH_{sol}), a suitable heating or cooling can guarantee that the temperature of the solution flowing along the membrane is high or low enough to be always under saturation condition. For the crystals of interest in this work (NaCl and $\text{MgSO}_4 \times 7\text{H}_2\text{O}$), both characterized by a positive enthalpy change of solution, a heating guarantees that the temperature of the solution flowing along the membrane is high enough to avoid crystals formation inside the membrane module.

Moreover, once the crystals are formed, they are removed from MCr lab plant through a so-called *crystals recovery system*, thus avoiding their deposition and/or accumulation inside the plant. The *crystals recovery system* has been designed and built in the laboratory and it is mainly constituted by two COLE PARMER—MASTER-FLEX L/S pumps and a filtration unit. The first pump withdraws some of the solution from the crystallization tank and sends it to the filtration unit. The latter keeps on a filter the achieved salts. The filtered liquor, through the second pump, is sent to the membrane module in order to be further concentrated. In Fig. 2 the schematic

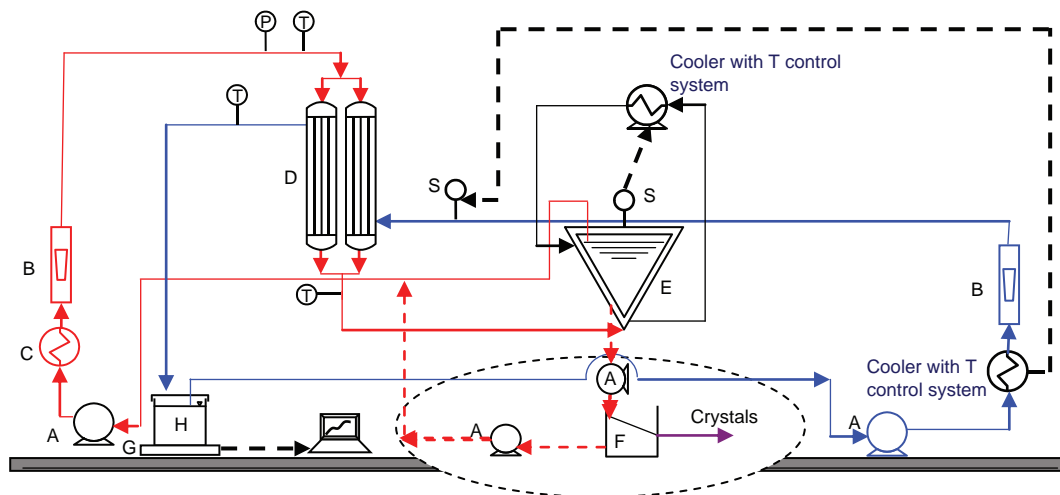


Fig. 2. Schematic flow sheet of the MCr lab plant: (A) pump; (B) flow-meter; (C) heater; (D) membrane module; (E) crystallizer tank; (F) crystals separation system; (G) balance; (H) distillate tank; (P) manometer; (T) thermocouples; (S) external temperature sensor.

flow sheet of the adjusted MCr lab plant is shown. In the figure the dotted area represents the *crystals recovery system* for the removal of the produced salts.

In the plant the control of the temperature inside the crystallization tank occurs through the use of NESLAB RTE 17 refrigerated bath supplied with external temperature sensor. The estimation of the trans-membrane flux occurs by evaluating weight variations in the distillate tank with a Reflex HP 8200 balance. The control of the trans-membrane flux is realized through the use of a computer which acquires instantaneously the data from the balance. Therefore, the balance represents the system both for data acquisition and, connected to the computer, for the control of the stability of the crystallization process. In fact, the balance has the following functions:

- it records the time variations of the distillate volume that it is collected in the permeate tank;
- it transfers the weight data to the computer which, through the use of an appropriate software, estimates the trans-membrane flux and shows to the users its graphic trend vs time. An eventual precipitation and/or accumulation of crystals on membrane surface is immediately seen by the operators through a drop of the trans-membrane flux.

3. Results and discussion

3.1. Concentration tests: trans-membrane flux measurements and analysis of the produced crystals

Figure 3 shows the trend of trans-membrane flux with time obtained during lab tests at two different retentate flow rates and constant temperature, and using as MCr feed the NF retentate. In both cases, apart an initial transitory stage, trans-membrane flux has shown

almost a constant trend. As discussed earlier, the constant trend is characteristic of a good operation because means no crystals deposition inside the membrane module. This happens because the temperature of feed and the thermal difference between the two streams are high enough to contain the decrease in driving force due to concentration rise. Moreover the slight decrease in trans-membrane flux observed when the crystals were formed has been solved putting into operation the *crystals recovery system*. This tool has allowed to separate the produced salts from the crystallizing solution: the crystals are kept on the paper filter while the remaining solution is sent to the membrane modules in order to be further concentrated.

Figure 4 shows that the trans-membrane flux increases with the temperature of the retentate. This trend is characteristic of a temperature driven membrane operation (as MCr) in which the driven force grows when the temperature of the feed and/or the trans-membrane temperature difference increase.

Moreover, the influence of retentate flow rate and temperature appears evident in the time for reaching supersaturation and crystals formation: it decreases when these parameters increase (Table 2).

For what concerns the type of produced crystals, they have been analyzed by scanning electronic microscopy, energy dispersive X-ray (EDX), low temperature differential scanning calorimeters (DSC) and Fourier transform infrared spectroscopy (FT IR) methods:

1. the low temperature DSC measures on the achieved crystals (maximum temperature 250°C) clearly showed that no $\text{MgCl}_2 \cdot 6\text{H}_2\text{O}$ was formed during the MCr tests of NF/RO retentate;
2. the EDX (recorded using a Philips EDAX analysis system) and FT IR (recorded using a Perkin

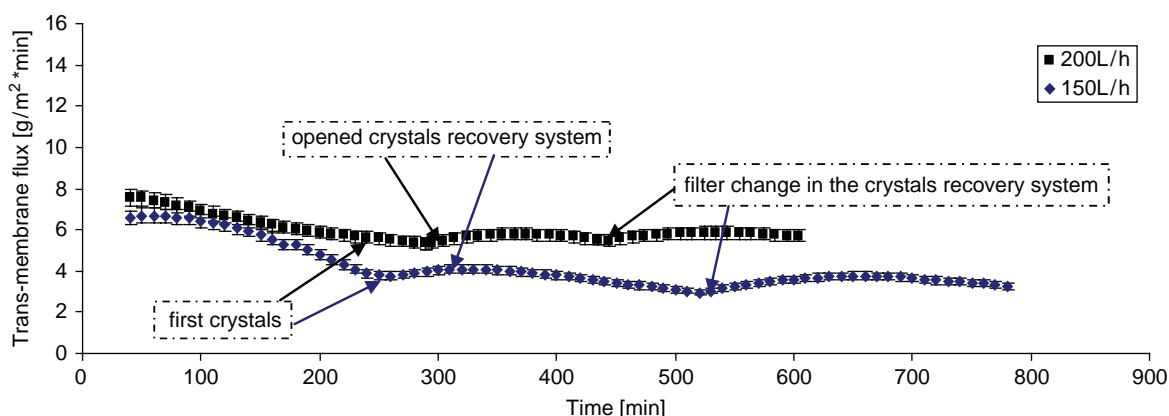


Fig. 3. Trans-membrane flux vs time at different retentate flow rates and constant temperature ($T_{\text{feed, retentate side}} = 34 \pm 1^\circ\text{C}$; $T_{\text{feed, permeate side}} = 16 \pm 2^\circ\text{C}$).

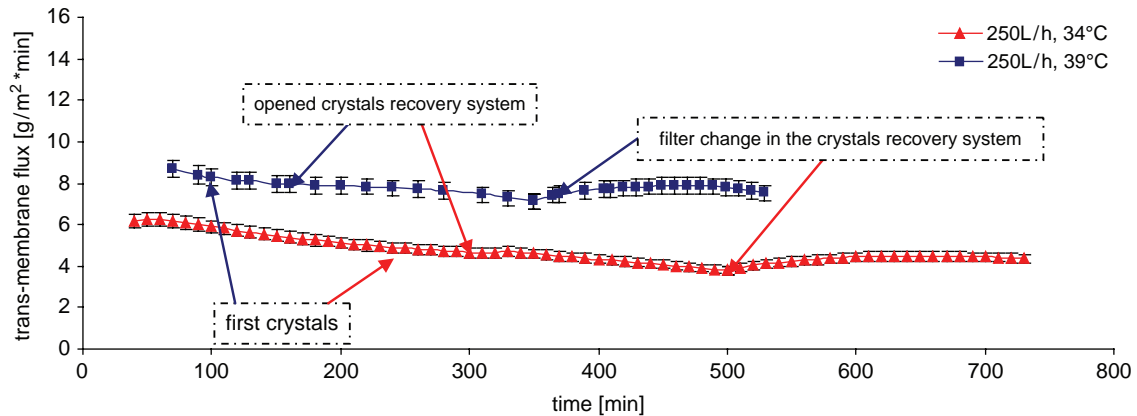


Fig. 4. Trans-membrane flux vs time at different retentate temperature and constant flow rate (retentate flow rate = 250 L/h).

Table 2

Time for reaching crystals formation.

Flow rate [L/h] and temperature [°C] of the retentate	Time for reaching crystals formation [min]	Flow rate [L/h] and temperature [°C] of the retentate	Time for reaching crystals formation [min]
120 L/h and 34 ± 1°C	230	120 L/h and 39 ± 1°C	150
200 L/h and 34 ± 1°C	190	200 L/h and 39 ± 1°C	140
250 L/h and 34 ± 1°C	160	250 L/h and 39 ± 1°C	100

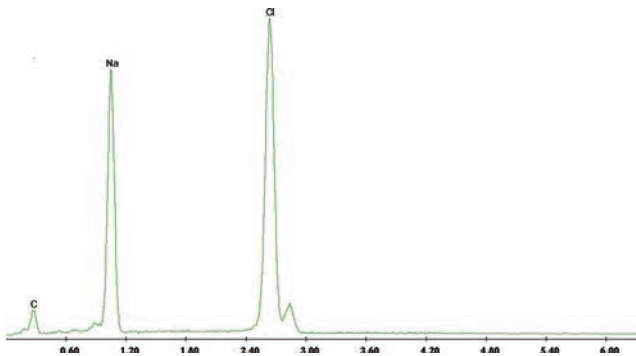


Fig. 5. EDX spectrum of produced NaCl crystals from the crystallization of NF retentate.

Elmer—spectrum one model FT IR spectrometer) analysis proved the formation of NaCl from RO retentate. Both NaCl and epsomite have been found in the salts produced from the crystallization of NF retentate (Figs. 5 and 6).

3.2. Crystallization tests: product characterization

During crystallization runs, suspension samples were withdrawn from the retentate tank every 30 min,

particles filtered and examined visually in order to determine CSD. Knowledge of the evolution of particle size distribution as function of time allows to evaluate quality, CV, middle diameter (d_m) and growth rate of the produced crystals and to test the fluid-dynamic effect on MCr operation and, in particular, on crystals growth rate.

The CSD of the crystals contained in a known volume of magma was measured by screen analysis performed via an optic microscope (ZEISS, model Axiovert 25) and pictures recorded with a video-camera module VISIOSCOPE Modular System equipped with optical head (10/100X).

Crystal size distribution is one of the main characteristics of a crystalline product. Crystal size distribution is important for the product quality, but also it influences the performance of the process, the separation of the crystals from the mother liquor and the subsequent drying of the crystals. It is also essential for the storage and handling of the final product. In general, both for small and large crystals, a narrow distribution around the mean crystal size is required.

Figure 7 shows the trend of CSD for the NaCl crystals produced in one of the carried out MCr test with RO retentate. The evolution of CDS shows that the initial peak of the distributions moves towards the larger dimensions as a consequence of the crystals growth.

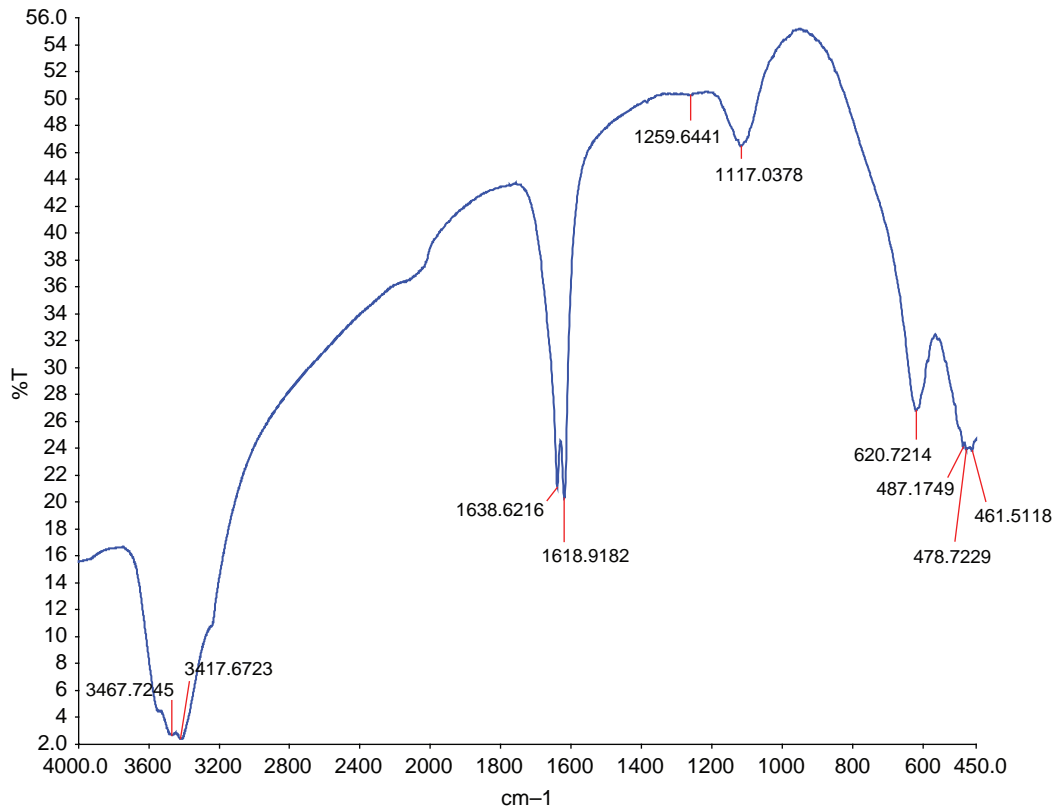


Fig. 6. FT IR spectrum of some of the achieved epsomite crystals from the crystallization of NF retentate.

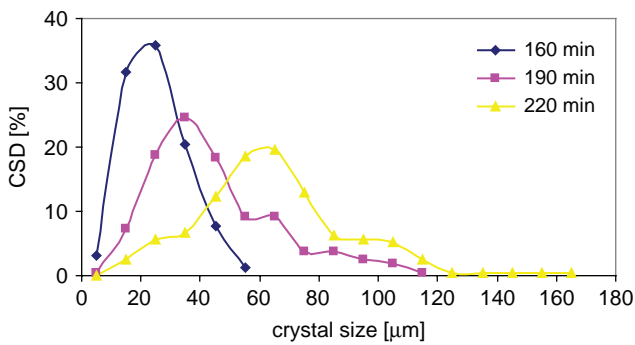


Fig. 7. CDS for NaCl crystals produced from RO retentate. MCr operative conditions: feed flow rate = 120 L/h; temperature at the module entrance for retentate and permeate side constant and equal to $35 \pm 1^\circ\text{C}$ and $16 \pm 2^\circ\text{C}$ respectively.

Crystal size distribution allows to evaluate the cumulative percent function and the CV [8]:

$$CV = \frac{\text{standard deviation}}{\text{mass based mean size}} = 100 \frac{PD_{84\%} - PD_{16\%}}{2 \cdot PD_{50\%}} \quad (1)$$

where PD is the crystal length at the indicated percentage.

Experimental data relative to the cumulative fractional distribution of averaged slurry samples as a

function of the particle size are shown in Fig. 8 at three different operative conditions (details are reported in the Table 3).

By giving the CV and the mean particle diameter, a description of the particle-size distribution is obtained which is normally satisfactory for most industrial purposes. Some experimental evaluations of the CV and of the middle diameter (d_m) as obtained in the carried out NF retentate and RO retentate crystallization tests are reported in Tables 4 and 5, respectively.

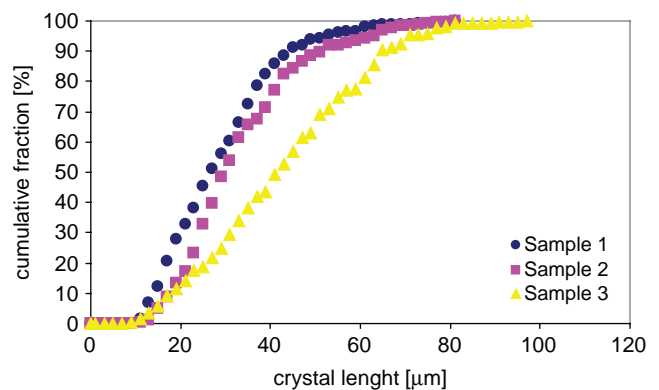


Fig. 8. Cumulative distribution of crystals per unit of volume vs particle size at operative conditions indicated in Table 3.

Table 3

Operative conditions for the crystals samples whose cumulative distributions are shown in Fig. 8. M = density of the crystal slurries.

MCr feed		NF retentate
Retentate flow rate		150 L/h
Retentate temperature		$39 \pm 1^\circ\text{C}$
Permeate flow rate		100 L/h
Permeate temperature		$16 \pm 2^\circ\text{C}$
	time [min]	M [g/L]
Sample 1	130	4.6
Sample 2	160	5
Sample 3	190	10.1

If crystals are removed from a mixed-suspension crystallizer, widely employed in the industrial crystallization, the CV should have a value of approximately 50% [8]. Low CVs, like those achieved in the carried out MCr tests and reported in Tables 4 and 5, are characteristic of narrow CSDs and, therefore, of a better product [9].

Moreover, NaCl crystals produced from NF retentate (Table 4) are characterized by lower coefficients of variation and middle diameters than those achieved from the crystallization of RO brine (Table 5). This is probably due to the fact that, in the crystallization of NF brine, the temperature of the MCr feed has been kept higher than that used in the crystallization of RO brine and this is expected to cause a higher dissolution of the smaller particles.

Table 4

Evolution in function of time of CV and middle diameter (d_m) determined from the experimentally obtained CSDs at three different MCr feed flow rate.

120 L/h			150 L/h			250 L/h		
time [min]	d_m [μm]	CV [%]	time [min]	d_m [μm]	CV [%]	time [min]	d_m [μm]	CV [%]
150	25.31	34.38	130	29.55	43.52	100	30.35	25.00
180	22.36	35.00	160	33.64	38.33	130	38.68	45.59
210	29.61	26.72	190	43.28	47.62	160	44.46	39.09

MCr feed = NF retentate; $T_{\text{feed, retentate side}} = 39 \pm 1^\circ\text{C}$; $T_{\text{feed, permeate side}} = 16 \pm 2^\circ\text{C}$.

Table 5

Coefficient of Variation and middle diameter (d_m) determined from the experimentally obtained CSDs at four different MCr feed flow rate.

120 L/h			150 L/h			200 L/h			250 L/h		
time [min]	d_m [μm]	CV [%]	time [min]	d_m [μm]	CV [%]	time [min]	d_m [μm]	CV [%]	time [min]	d_m [μm]	CV [%]
220	64.7	42.6	211	56.3	36.8	214	65.1	49.1	200	64.8	42.3

MCr feed = RO retentate; $T_{\text{feed, retentate side}} = 35 \pm 1^\circ\text{C}$; $T_{\text{feed, permeate side}} = 16 \pm 2^\circ\text{C}$.

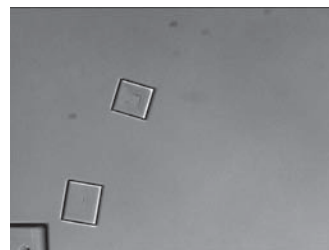


Fig. 9. NaCl crystalline habit. (MCr feed = NF retentate; retentate flow rate = 250 L/h; $T_{\text{feed, retentate side}} = 39 \pm 1^\circ\text{C}$; $T_{\text{feed, permeate side}} = 16 \pm 2^\circ\text{C}$). Picture from optical microscope, magnification: X10.

For what concerns the shape of the produced NaCl crystals, they showed the characteristic cubic block-like form in accordance with the expected geometry of the NaCl crystals when examined visually with the optic microscope (Fig. 9).

However, in each sample, a small fraction of particles exhibiting an elongated shape was present. Therefore, the length/width ratio of each produced crystal has been determined and the achieved results (reported in the histograms of Figs. 10 and 11) have shown that the most part of particles had a length/width ratio in the range 1.0–1.2, that is to have almost a cubic shape.

The percentage of NaCl crystals exhibiting an elongated shape was higher in the crystallization of NF retentate than in the crystallization of RO retentate. This is probable due to the presence, in the crystallization of NF brine, of a bigger concentration of ions different from Na^+ and Cl^- (such as Mg^{2+} , SO_4^{2-} , etc.) which might act as impurities.

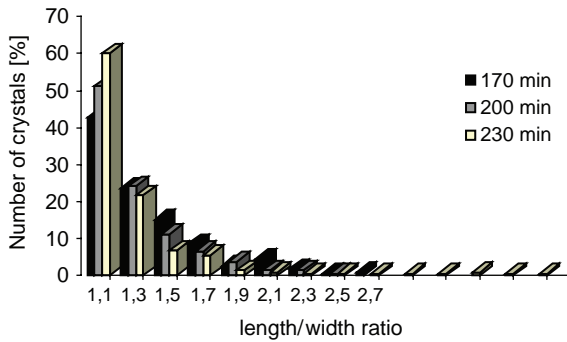


Fig. 10. Number of crystals [%] vs length/width ratio (MCr feed = RO retentate; $T_{\text{feed, retentate side}} = 35 \pm 1^\circ\text{C}$; $T_{\text{feed, permeate side}} = 16 \pm 2^\circ\text{C}$; Retentate flow rate = 100 L/h).

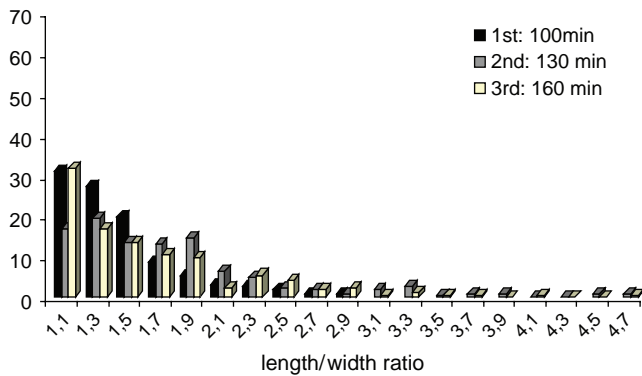


Fig. 11. Number of crystals [%] vs length/width ratio (MCr feed = NF retentate; $T_{\text{feed, retentate side}} = 39 \pm 1^\circ\text{C}$; $T_{\text{feed, permeate side}} = 16 \pm 2^\circ\text{C}$; Retentate flow rate = 250 L/h).

3.3. Crystallization kinetics

The Randolph–Larson general-population balance has been applied in order to predict growth rates based on the experimental population density data [10].

The Randolph–Larson general-population balance, valid for a steady-state crystallizer receiving solids-free feed and containing a well-mixed suspension of crystals experiencing negligible breakage, is as follows:

$$\frac{dn}{dL} + \frac{n}{Gt} = 0 \quad (2)$$

where n , crystal population density; L , crystal size; G , growth rate; t , retention time.

Equation (2) is applicable if the delta L law applies (i.e., G is independent of L) and the retention time is assumed to be invariant and calculated as $t = V/Q$ (V = volume and Q = flow rate). Integrated between the limits n^0 (the population density of nuclei for which L is assumed to be zero) and n (that of any chosen crystal size L), Eq. (2) becomes:

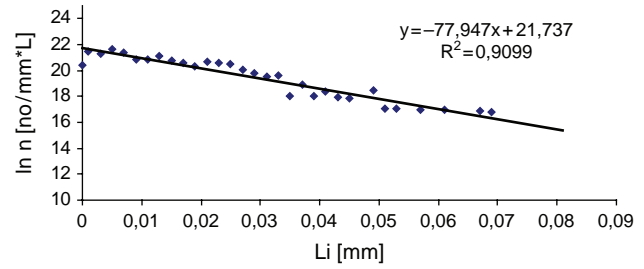


Fig. 12. Population-density plot for NaCl crystals produced from NF brine (retentate flow rate equal to 150 L/h and retentate temperature equal to $39 \pm 1^\circ\text{C}$).

$$\int_{n^0}^n \frac{dn}{n} = \int_0^L \frac{dL}{Gt} \Rightarrow \ln n = \frac{-L}{Gt} + \ln n^0 \text{ or } n = n^0 e^{-L/Gt} \quad (3)$$

Thus, a plot of $\ln n$ vs L is a straight line whose intercept is $\ln n^0$ and whose slope is $-1/Gt$.

Figure 12 reports the estimated population density data vs crystal size for a representative set of averaged samples at $t = 130$ min and $M = 4.6$ g/L; a linear regression of equation $n = n^0 \cdot \exp(-L/Gt)$ is used to determine both the crystals growth rate G and the nuclei population density n^0 .

From several other samples taken from the crystallizer during the same test and for each carried out run, a plot of growth rate G vs feed flow rate can be constructed in order to study the fluid-dynamic effect on MCr operation.

Crystal growth rate is generally recognised as a layer-by-layer process and, since growth can occur only at the face of the crystal, material must be transported to that face from the bulk of the solution. Diffusional resistance to the movement of molecules (or ions) to the growing crystal face, as well as the resistance to integration of those molecules into the face, must be considered. In the first case, G increases with the feed flow rate due to the improvement of the transport coefficients; in the second case, G decreases when feed flow rate increases because a high flow rate disturbs the molecular organization which precedes the integration into crystal lattice.

The trend of NaCl crystals growth rate vs flow rate for the particles produced from the crystallization of both RO retentate and NF retentate is reported in Figs. 13 and 14 respectively.

For what concerns NaCl crystals obtained from RO brine, according to the experimental results (Fig. 13), until a feed flow rate equal to about 150 L/h crystals growth rate is limited by the integration of molecules into crystal lattice; then, for higher feed flow rate, mass-diffusion is the control based mechanism.

For NaCl particles achieved from the crystallization of NF brine, the obtained trend of the crystals growth

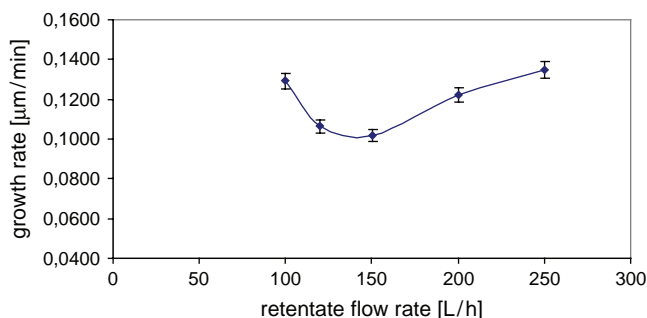


Fig. 13. Growth rate vs retentate flow rate for NaCl particles produced from the crystallization of RO brine.

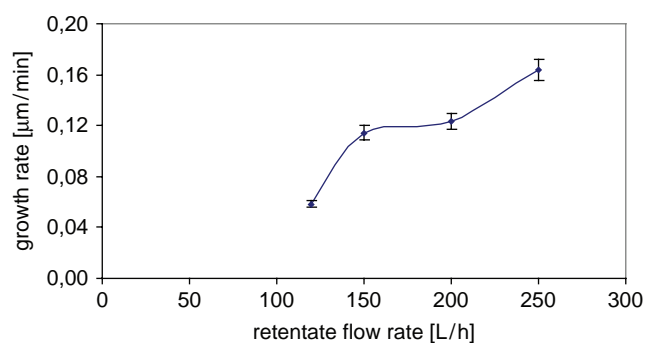


Fig. 14. Growth rate vs retentate flow rate for NaCl particles produced from the crystallization of NF brine.

rate vs feed flow rate (Fig. 14) has proved that, in this case, crystals growth is limited by the diffusional resistance to the movement of molecules to the growing crystal face.

The higher values of growth rate obtained in the tests on NF brine can be explained by considering that kinetic rates and thermodynamic solubility equilibrium, as well as shape and purity of crystals, strongly depend on the presence of different components in the crystallizing solutions, degree of supersaturation, temperature and hydrodynamic conditions. In fact, [8] reports that NaCl growth rate and hardness increase in presence of other salts (range of concentration 0–100 ppm).

4. Effect of humic acid on membrane crystallization process

Natural waters contain natural organic matter (NOM), largely composed of humic substances, which are macromolecular mixtures of humic acid (HA), fulvic acids and humin. The removal of NOM from feed water is necessary in potable water production because it is responsible for colour in the water, formation of

carcinogenic disinfection by products during water disinfection, complexation with heavy metals and calcium, etc.

Membrane processes have been shown to remove NOM effectively from water [11]: in the ultrafiltration of water containing HAs, the retentions were in the range of 85–90%; NOM removal by NF membranes, quantified by total organic carbon (TOC) rejection, was found to be more than 90% at pH 8.

However, membrane fouling by NOM is one of major obstacles limiting the use of these processes. The observed fouling leads to a decrease of the membrane performance and subsequently to a reduction of the membrane life. The membrane surface characteristics (i.e. hydrophobicity, porosity, etc.), the hydrodynamic conditions (i.e. transmembrane pressure, crossflow velocity, temperature, etc.) and the chemical composition of feed liquid (i.e. pH, ionic strength, type of NOM, etc.) exert significant effects on membrane fouling [12].

Interest of the work presented in this section is to study membrane fouling in MCr process when applied to waters containing HA and inorganic salts similarly to NF brine of a seawater desalination plant. The effect of HAs on crystals growth is also included.

4.1. Effect of humic acid on membrane crystallization.

Trans-membrane flux and crystals growth measurements

Figure 15 reports the effect of HA on trans-membrane flux during MCr process. In particular, the tests have been carried out on solutions with the same composition of the NF brine after the precipitation with anhydrous sodium carbonate previously described in which HA has been added.

Humic acid concentrations have been evaluated by using TOC Analyzer Shimadzu TOC-Vcsn.

The achieved results have proven that trans-membrane flux decreases when the concentration of HA increases due to the formation of a fouling layer. In fact, in agreement with what found in literature, the examination of the membrane surface confirmed the existence of a fouling layer which appeared dark brown.

The deterioration of flux due to the fouling layer may be attributed to two effects: first, the reduction of surface area available for vaporization as the fouling layer blocked the pore entrances; second, the fouling layer may decrease the heat transfer driving force.

Moreover, dissolved HA has influenced also the dimensions and the kinetics of salts precipitation (Tables 6 and 7).

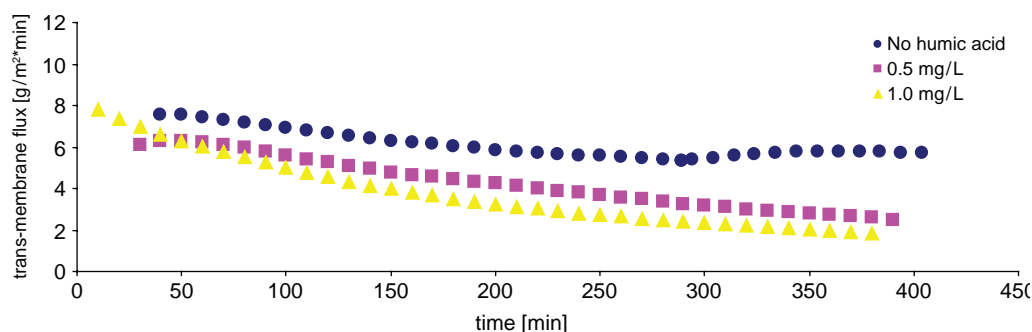


Fig. 15. Trans-membrane flux vs time for NF retentate with different HA concentrations. $\Delta T_{in} = 11^{\circ}\text{C}$, $\Delta T_{out} = 9^{\circ}\text{C}$, retentate flow rate = 207 L/h, $T_{in, feed} = 39 \pm 1^{\circ}\text{C}$.

Table 6

Evolution in function of time of the CV and middle diameter (d_m). Parameters determined from the experimentally obtained CSDs at two different HA concentrations.

Humic acid concentration [mg/L]					
0.5			1.0		
Sample n°	d_m [μm]	CV [%]	Sample n°	d_m [μm]	CV [%]
1	17.48	41.12	1	16.32	41.67
2	24.22	41.67	2	19.68	48.57
3	33.49	43.33	3	37.02	67.19

Retentate flow rate = 207 L/h; permeate flow rate = 100 L/h; $T_{feed, retentate side} = 39 \pm 1^{\circ}\text{C}$.

Some experimental evaluations of the CV and the middle diameter (d_m) as obtained in the carried out NF retentate crystallization tests at different HA concentrations are reported in Table 6. These can be compared to the results obtained in the crystallization of NF retentate without HA (Table 4) showing higher d_m (values vary between 22.36 and 44.46 μm) and smaller CVs (values vary between 25% and 45.59%).

Table 7 reports the crystals growth rate G and the nuclei population density n^0 as experimentally achieved at different HA concentrations.

In conclusion, the effect of HA is not only on membrane fouling but also on crystals size (smaller particles), on CV (higher CVs, characteristic of wider distributions around the mean crystal size) and on crystals growth rate which is at least one order of magnitude smaller than the one obtained from inorganic NF brine solutions (Fig. 14).

Table 7

Crystals growth rate G and nucleation rate at different HA concentration.

Humic acid concentration [mg/L]	0.5	1.0
G [$\mu\text{m}/\text{min}$]	0.0407	0.0612
$\ln n^0$	21.75	21.87

The achieved results agree with Zuddas observations [13] on calcite precipitation from seawater solution. It was found that the dissolved organic matter in the form of HA inhibits the rate of calcite crystal growth in strong electrolyte solutions of ionic strength like seawater.

5. Conclusions

In this paper the proper functioning of membrane crystallizer and its potentialities for the exploitation of some components contained in the NF and RO streams of the desalination plants have been analysed.

The first objective of the work has been the identification of appropriate measures for preventing crystals deposition on membrane surface and inside the membrane module. In the used lab plant, this problem has been controlled by recovering the produced crystals and by controlling the temperature of the solution flowing along the membrane module. The obtained almost constant trend of the trans-membrane flux has been the demonstration of the good carried out operations.

The experimental tests have also allowed to test fluid-dynamic effect on MCr operation and, in particular, on trend of solvent transmembrane flux and crystals

growth rate. Crystals distribution has been characterized by the CV and middle diameter d_m . The kinetic parameters have been investigated by using a mathematical model for continuous crystallizers of the mixed-suspension or circulating-magma type.

The achieved results have shown that transmembrane flux increases with retentate flow rate and temperature. Therefore, the time for reaching supersaturation and crystals formation decreases when these parameters rise. The obtained CVs are lower than those from conventional equipments and are therefore characteristic of narrow CSDs and of qualitatively better products.

Moreover, the experimentally determined crystals growth rate has shown that the presence of ions accelerate kinetic rate of NaCl crystallization while the presence of HA in NF retentate inhibits crystals growth rate.

From here the necessity to optimize the NF/RO pre-treatment steps in order to control the crystallization kinetics that are linked with the nature and the amount of the foreign species existing in the highly concentrated brines emerging from the NF and RO stages. These substances, besides causing fouling on RO membranes, can easily hinder the crystallization kinetics, thus leading either to the cessation of growth or to the production of a product exhibiting inferior, undesired properties.

In conclusion, the use of membrane crystallizers on NF and/or RO brine and the choice of a suitable NF/RO pre-treatment might offer the possibility of producing solid materials of high quality, whose structures (polymorphism) and morphologies (size, size distribution, shape, habit) can be adequate to represent a valuable

by-product, transforming the traditional brine disposal cost in a potential new profitable market.

Acknowledgements

The authors acknowledge the financial support of the European Commission within the 6th Framework Program for the grant to the membrane-based desalination: an integrated approach (MEDINA) project. Project no.: 036997.

References

- [1] T.E. Borgate, Published by Murray–Darling Basin Commission, Canberra City, Australian Capital Territory (2004) (web-site: http://www.mdbc.gov.au/_data/page/334/MDBCintroduction.pdf).
- [2] M. Turek, *Desalination*, 153 (2002) 173–177.
- [3] E. Curcio, A. Criscuoli and E. Drioli, *Ind. Eng. Chem. Res.*, 40 (2001) 2679–2684.
- [4] E. Drioli, E. Curcio, A. Criscuoli and G. Di Profio, *J. Membrane Sci.*, 239 (2004) 27–38.
- [5] F. Macedonio, E. Curcio and E. Drioli, *Desalination*, 203 (2007) 260–276.
- [6] F. Macedonio, E. Drioli, E. Curcio and G. Di Profio, *Desalination Water Treatment*, 9 (2009) 49–53.
- [7] P. Dydo, M. Turek and J. Ciba, *Desalination*, 159 (2003) 245–251.
- [8] J.H. Perry and D. Green, *Perry's chemical engineers' handbook*, McGraw-Hill International Editions, New York, 1987.
- [9] E. Curcio and E. Drioli, *Separation Purification Rev.*, 34 (2005) 35–85.
- [10] A.D. Randolph and M.A. Larson, *Theory of particulate processes*, Academic Press, New York, 1971.
- [11] S. Srisurichan, R. Jiraratananon and A.G. Fane, *Desalination*, 174 (2005) 63–72.
- [12] M. Khayet and J.I. Mengual, *Desalination*, 168 (2004) 373–381.
- [13] P. Zuddas, K. Pachana and D. Faivre, *Chem. Geol.*, 201 (2003) 91–101.